Archival Report

Biological Psychiatry: CNNI

In Trauma-Exposed Individuals, Self-reported Hyperarousal and Sleep Architecture Predict Resting-State Functional Connectivity in Frontocortical and Paralimbic Regions

Jeehye Seo, Katelyn I. Oliver, Carolina Daffre, Kylie N. Moore, Natasha B. Lasko, and Edward F. Pace-Schott

ABSTRACT

BACKGROUND: Symptoms of posttraumatic stress disorder (PTSD) reflect abnormalities in large-scale brain networks. In individuals with recent trauma exposure, we examined associations of seed-based resting-state functional connectivity (rs-FC) with posttraumatic symptoms and sleep. We hypothesized that more severe PTSD symptoms and poorer sleep quality would predict 1) greater rs-FC between fear-related seeds and other fear-related regions and 2) lesser rs-FC between fear-related seeds and emotion-regulatory regions.

METHODS: Seventy-four participants who had experienced a DSM-5 criterion A stressor within the past 2 years and ranged from asymptomatic to fully meeting criteria for PTSD diagnosis underwent 14 days of actigraphy and sleep diaries, a night of ambulatory polysomnography, and a functional magnetic resonance imaging resting-state scan at 3T. rs-FC measures of 5 fear-related seeds and 1 emotion regulatory seed with regions of the anterior cerebrum were correlated with PTSD symptoms, objective and subjective habitual sleep quality, and sleep architecture.

RESULTS: Longer objective habitual sleep onset latency was associated with greater connectivity between fear-related seeds and other regions of the salience network. Greater PTSD symptoms were associated with less connectivity between fear-related seeds and anterior emotion regulatory regions, whereas greater percent slow wave sleep was associated with more connectivity between these regions. However, other objective and subjective measures reflecting better habitual sleep quality were associated with less rs-FC between these regions.

CONCLUSIONS: Longer sleep onset latency predicted greater rs-FC among fear-related areas. More severe PTSD symptoms predicted less rs-FC between fear and fear regulatory regions reflecting putatively reduced top-down fear regulation. Some (e.g., percent slow wave sleep), but not all sleep indices predicted greater top-down fear regulation.

Keywords: Emotion regulation, Hyperarousal, PTSD, Resting-state functional connectivity, Salience network, Trauma

https://doi.org/10.1016/j.bpsc.2019.06.013

Sleep disturbances, such as insomnia and nightmares, are ubiquitous and debilitating symptoms of posttraumatic stress disorder (PTSD) and are associated with substance abuse, depressive symptoms, and suicidal ideation (1–4). PTSD is associated with increased threat sensitivity and fear generalization as well as deficits in attentional control and fear extinction (5–14). Such functions are controlled by anterior forebrain circuits involving the amygdala, insula, prefrontal cortex (PFC), and hippocampus (8,15) and have been shown to be sensitive to sleep disruption (16–19). It is increasingly understood that psychiatric disorders such as PTSD are disorders of specific neural pathways (15,20,21). Resting-state functional connectivity (rs-FC), an effective way to understand network connectivity, is an imaging method that exploits low-frequency oscillations (0.008−0.1 Hz) of the blood oxygen level–dependent (BOLD) functional magnetic resonance imaging (fMRI) signal during resting wakefulness. It is used to investigate relationships between large-scale intrinsic spontaneous brain activity in different regions (22–25) and has successfully defined at least 7 widely distributed, stable brain networks (26–28). These 7 networks include the default mode network (DMN), the salience network, a central executive network, a dorsal attention network, and 3 networks corresponding to processing in the major sensory modalities (28–31).

Studies using rs-FC have identified brain regions with altered activity and connectivity in individuals with PTSD compared with healthy subjects with and without previous

SEE COMMENTARY ON PAGE 1018

ISSN: 2451-9022

trauma exposure. For example, using a region of interest (ROI) approach, Nicholson *et al.* (32) showed differences between individuals with PTSD and dissociative symptoms, individuals with PTSD without dissociative symptoms, and healthy control subjects in rs-FC between insular subregions and the basolateral amygdala. Olson *et al.* (33) examined rs-FC between dorsolateral PFC and anterior and posterior DMN seeds in individuals with PTSD, trauma-exposed control subjects with no PTSD, and control subjects with no exposure to trauma, finding greater anticorrelation between dorsolateral PFC and posterior DMN (precuneus) in subjects with PTSD compared with other groups. When comparing an amygdala seed in a small sample of male veterans with PTSD with combat-exposed control subjects (34), veterans with PTSD showed greater amygdala-insular and lesser amygdala-hippocampal rs-FC. In a qualitative review of 9 seed-based studies, Koch *et al.* (35) reported greater rs-FC within the salience network and less rs-FC within the DMN in subjects with PTSD compared with control subjects.

The current study adopts the Research Domain Criterion approach (20,36,37) whereby a specific population is examined dimensionally across a range of both normal and abnormal values of specific symptoms. In this case, adults with recent exposure to trauma were examined across a range of sleep quality and PTSD symptom variables. Additionally, rather than specify individual target ROIs in addition to seed ROIs, we examined rs-FC between 6 symptom-relevant seeds and the entire anterior cerebrum. Five fear-related seeds were areas of the salience network believed to be important in fear expression, whereas the sixth seed, the ventromedial PFC (vmPFC), is a portion of the anterior DMN believed to exert top-down inhibition of fear (14). Although studies comparing resting neuronal activity levels between individuals with PTSD and control subjects have identified differences in posterior regions (35,38,39), seed-based rs-FC studies have focused on anterior regions (see above). Moreover, major elements of emotion generation and emotion regulatory networks as well as key nodes of fear expression and fear extinction networks that are known to display task-based abnormalities in PTSD all are anteriorly localized (8,14,40,41). Higher-level, cognitively based emotion regulatory structures, such as the lateral PFC (42), may exert control over subcortical generators by recruiting midline limbic cortices, such as the vmPFC (43).

We thus formed 2 hypotheses. Hypothesis 1 suggested that greater PTSD symptoms and poorer sleep quality (including nightmares) would predict greater rs-FC among fear-related seeds and other regions of the salience network. Hypothesis 2 suggested that greater PTSD symptoms and poorer sleep quality would predict less rs-FC between fear-related seeds and prefrontal regions related to cognitive control (central executive network) and emotion regulation in lateral and medial PFC areas, the latter including the vmPFC and dorsomedial PFC (dmPFC). A corollary of hypothesis 2 was that fewer PTSD symptoms and better sleep quality would also predict greater rs-FC between the vmPFC seed and central executive network and medial PFC areas, indicating a putatively greater coordination among areas subserving emotional and cognitive control.

METHODS AND MATERIALS

Participants

Using online and posted advertisements, 74 right-handed participants ranging from 18 to 40 years of age (mean ± SD 23.5 ± 4.5) (Table 1) were recruited from the Boston metropolitan area. All participants had experienced a DSM-5 criterion A traumatic event (index trauma) in the past 2 years. Potential participants first completed a telephone screening, and individuals who qualified completed psychiatric and sleep interviews. Current and lifetime history of DSM-IV-TR Axis I psychiatric disorders were evaluated using the Structured Clinical Interview for DSM-IV for Non-Patients (44), and PTSD symptoms were assessed using the Clinician-Administered PTSD Scale for DSM-5 (45) and the PTSD Checklist for DSM-5 (PCL-5) (46). See the Supplement for descriptions of the sleep disorders evaluation and exclusion criteria. All study procedures were approved by the Partners Healthcare Institutional Review Board. All participants provided written informed consent and were paid for their participation.

Psychopathology Severity Indices

The PCL-5 was used to measure overall PTSD severity. A composite hyperarousal index (CHI) was calculated from the hyperarousal (cluster E) items from the Clinician-Administered PTSD Scale for DSM-5 and the PCL-5 by first converting each assessment's hyperarousal item totals to a 0–100 scale and then averaging these 2 scores (Table 1; Supplemental Methods).

Habitual Sleep Monitoring Period and Questionnaires

Participants underwent an approximately 2-week (mean 14.6 ± 2.9 nights) sleep assessment period with wrist actigraphy and sleep diaries that also contained a nightmare questionnaire. Following an acclimation/sleep disorders diagnostic night using ambulatory polysomnography (PSG), ambulatory PSG was repeated on the night before the resting-state fMRI scan. No participants were excluded for obstructive sleep apnea or periodic limb movements during sleep sufficient to warrant referral for treatment. Additionally, participants were prohibited from consuming alcohol or recreational drugs throughout this period and instructed to not consume caffeine or take daytime naps the day before or the day of their scan. During the sleep monitoring period, participants completed an online battery of questionnaires (Table 1).

Actigraphy and Sleep Diaries

During the 2-week sleep assessment period, participants continuously wore the Actiwatch-2 (Philips Respironics, Bend, OR) and pressed an event marker before attempting to sleep in the evenings and when they first woke up in the morning. Event markers were used to time stamp the time in bed. Within this period, the default algorithm of Actiware 5.61 software (Philips Respironics) determined total sleep time (TST), sleep onset latency (SOL), and sleep efficiency (SE) (TST in minutes divided by time in bed) (Table 1). Actiwatch SOL and SE estimates have been validated with in-laboratory PSG and are considered good estimates of these measures (47,48). When button

presses were missed, times recorded on diaries were substituted, which occurred 18.9% of the time. If both button presses and diary records were missing for a particular night, that night was excluded from the final analysis. Actiwatch data for 5 subjects were excluded owing to malfunction (n = 69). The Evening-Morning Sleep Questionnaire diary (49,50) provided subjective TST, SOL, and SE during the sleep monitoring period (Table 1; see Supplemental Methods for computation details). Evening-Morning Sleep Questionnaire data for 4 subjects were omitted owing to incomplete diaries (n = 70).

Dream Reports

On waking, 69 participants completed a dream questionnaire asking whether a dream was recalled, whether it was a nightmare (causing awakening) or a bad dream, and the degree to which it resembled their trauma (exactly, similar, possibly similar, or unrelated). Per-total-diary percentages for nightmares, bad dreams, the sum of bad dreams and nightmares, and the sum of dreams that were exactly like/similar to the trauma were calculated as nights with specific dream types divided by total nights studied.

Table 1. Demographic and Sleep Characteristics Among Total Sample of Trauma-Exposed Individuals (N = 74)

	Mean ± SD or n	Minimum Value	Maximum Value
Demographics			
Number of subjects	74		
Number of male subjects	25		
Age, years	23.5 ± 4.5	18	40
Educational Level			
High school or equivalent	5		
Some college	27		
Bachelor's (or associate's) degree	24		
Graduate degree	11		
Unknown or not reported	7		
PTSD Symptoms			
CAPS-5 total score	27.4 ± 16.6	0	58
PCL-5 total score[a]	36.6 ± 19.7	0	76
CHI (0–100 scale)[a,b]	28.8 ± 18.3	0	64.6
Time since trauma, months	12.3 ± 6.9	1	28
Sleep Questionnaires			
PSQI	7.13 ± 3.3	2	14
ESS	7.13 ± 4.7	0	19
MEQ	46.43 ± 9.6	25	68
Actigraph Data			
Total sleep time, min[a]	432.4 ± 51.5	299.7	538.9
Sleep efficiency, %[a]	90.7 ± 4.7	77.9	97.8
Sleep onset latency, min[a]	23.2 ± 18.8	2	86.2
Sleep midpoint, min after midnight[c]	290.3 ± 82.4	167.2	609
Sleep Diary Data			
Total sleep time, min[a]	432.5 ± 59.8	249.5	570.9
Sleep efficiency, %[a]	92.0 ± 6.1	66.5	99.2
Sleep onset latency, min[a]	22.5 ± 14.6	3	69.2
Number of dreams	6.2 ± 3.8	0	15
Number of nightmares and bad dreams	2.7 ± 2.8	0	13
Nightmares and bad dreams rate, %	48.4 ± 30.2	0	100
PSG Data			
Total sleep time, min	374.2 ± 124.5	48.5	635
N1%	6.5 ± 3.9	0.9	17.6
N2%	53.8 ± 9.9	21.8	70.5
Sleep onset latency	26.5 ± 39.1	0	255
REM latency	94.7 ± 48.1	0	243.5
Slow wave sleep, %[a]	21.6 ± 12.5	0.3	62.3
REM, %[a]	18.1 ± 6.9	0	42.1
Sleep efficiency, %[a]	85.2 ± 11.9	29.5	98.0

CAPS-5, Clinician-Administered PTSD Scale for DSM-5; CHI, composite hyperarousal index; ESS, Epworth Sleepiness Scale; MEQ, Morningness-Eveningness Questionnaire; PCL-5, PTSD Checklist for DSM-5; PSG, polysomnography; PSQI, Pittsburgh Sleep Quality Index; PTSD, posttraumatic stress disorder; REM, rapid eye movement.

[a]Predictor values selected pre hoc for resting-state functional connectivity analyses.

[b]CHI was calculated from the hyperarousal questions from CAPS-5 and PCL-5. Respective partial CAPS-5 and PCL-5 raw scores were first converted to a 0–100 scale, and then the 2 resulting values were averaged.

[c]Sleep midpoint was computed as the midpoint between sleep onset and final awakening (expressed as minutes past midnight).

Ambulatory PSG

The Somté PSG monitor (Compumedics USA, Charlotte, NC) was used with a standard montage (see Supplemental Methods for details). Sleep stage percentages, SOL, rapid eye movement sleep latency, and SE were computed from scored records. Owing to artifact in recordings, 13 subjects were excluded from final analyses (n = 61).

MRI Acquisition

Whole-brain images were collected with a 3T MAGNETOM Prisma scanner (Siemens Healthcare, Erlangen, Germany) and a 32-channel head coil. First, automated scout images and shimming procedures were performed to optimize field homogeneity. High-resolution 3-dimensional multiecho magnetization prepared rapid acquisition gradient-echo (T1-weighted) sequences (repetition time = 2530 ms; echo time 1, 2, 3, 4 = 1.69, 3.55, 5.41, 7.27 ms; flip angle = 7°) were collected with an in-plane resolution and slice thickness of 1.0 mm. Following these anatomical scans, 240 resting-state fMRI BOLD images were acquired with an interleaved T2*-weighted echo-planar imaging sequence. Forty-six slices per repetition time were obtained with the following parameters: 2.5-mm slice thickness, 3 × 3 mm in-plane resolution, repetition time = 2560 ms, echo time = 30 ms, flip angle = 90°. Total scan time was 10 minutes, and subjects were told to keep their eyes open and fixed on a white cross projected onto a screen.

Resting-State fMRI Data Analysis

MATLAB 2014a (The Mathworks, Inc., Natick, MA) and SPM8 (Wellcome Trust Centre for Neuroimaging; http://www.fil.ion.ucl.ac.uk/) were used to process BOLD images and perform statistical analyses on resting-state fMRI data. During preprocessing, functional images underwent slice timing, realignment, coregistration with the structural images, normalization into Montreal Neurological Institute space, and smoothing with an 8-mm full width at half maximum Gaussian kernel to increase the signal-to-noise ratio and account for between-subject anatomical variations.

rs-FC analyses were performed using CONN FC toolbox v.17c (http://www.nitrc.org/projects/conn) (51). All imaging data were bandpass filtered (0.008–0.09 Hz) to reduce low-frequency drift and noise effects, and physiological and other spurious noise sources in the BOLD signal were removed using the anatomical component-based noise correction (CompCor) strategy implemented in CONN (52). White matter signals, cerebrospinal fluid signals, and 6 motion-correction parameters obtained from the preprocessing procedure were also removed.

Following preprocessing, maps of FC were obtained by plotting the correlation strength between the mean time course of a seed region to that of each voxel using the seed-to-voxel analysis. Key nodes in fear and extinction networks were selected as seed regions. Five fear-related regions were selected, including the left and right amygdala, left and right anterior insula cortex (AIC), and dorsal anterior cingulate cortex (dACC). Additionally, 1 fear regulatory region in the vmPFC (14,53) was included for a total of 6 seed regions.

The amygdala and insular cortex seed regions were selected using parameters from the Automated Anatomical Labeling atlas (http://www.gin.cnrs.fr/en/tools/aal-aal2/) (54) and using the WFU PickAtlas software interface (http://fmri.wfubmc.edu/software/PickAtlas) (55). The vmPFC and dACC seed coordinates were chosen based on a meta-analysis of 298 fear-related studies from the NeuroSynth database (www.neurosynth.org) (56), and these were also employed in a previous seed-based rs-FC study (57). These seeds were defined by 6-mm-diameter spheres with peak coordinates for the vmPFC at [6, 40, −20]; dACC at [0, 14, 28]; left AIC at [−32, 16, −10]; right AIC at [38, 16, −10]; left amygdala at [−24, −4, −18]; and right amygdala at [26, 0, −22]. Although the vmPFC axial coordinate is positive, indicating right hemisphere laterality, the 6-mm sphere crosses the midline (axial coordinates from −1 to +9). Similarly, the 6-mm dACC sphere appears in both the left (−4) and the right (+4) hemispheres.

The mean time series for each seed region was calculated and then correlated with the time courses of each voxel throughout the whole brain. The resulting coefficients were converted to normally distributed scores using Fisher's *r*-to-*z* transformation to give maps of voxelwise FC for each seed ROI per participant. The value for each voxel represents its relative degree of FC to each seed (58). These maps were subsequently used for second-level analysis of relative FC using multiple regression analysis to investigate relationships of seed-to-voxel connectivity with psychopathology and sleep measures. To control for the potential effect of duration between trauma exposure and the start of the study, time since trauma (Table 1) was entered as a covariate of no interest along with age and sex.

In second-level analyses, correlation maps were restricted to an anterior cerebral mask (see Supplemental Figure S1 and its legend for specific regions). Although posterior regions might correlate meaningfully with sleep and hyperarousal variables, we chose this approach as a compromise between greatly restricting target ROIs (e.g., to only the seeds themselves) and whole-brain second-level analyses. Doing so, we increased statistical power by reducing the total number of voxels while continuing to examine the majority of putative emotion expression and regulatory regions. To rule out potentially meaningful correlations within posterior regions, we investigated seed–to–whole-brain connectivity and performed additional analyses (Supplement and Supplemental Table S2).

Corrections for multiple comparisons were conducted with nonparametric permutation analyses (SnPM) using a toolbox for SPM (http://warwick.ac.uk/snpm; SnPM13) (59) and the following steps. The results of second-level analyses were first thresholded at cluster-defining threshold $p < .001$. A more rigorous analysis using SnPM was then performed to determine which clusters contained sufficient numbers of contiguous voxels that the likelihood of familywise error (FWE) (type I error) for that cluster was $p < .1$ and $p < .05$ following 5000 permutations. Such nonparametric permutation analysis is a highly conservative adjustment determined to be the most effective for controlling FWE by Eklund *et al.* (60). Mean *z* scores of clusters showing significant correlation with psychopathology and sleep variables and surviving the SnPM FWE correction were extracted using the REX toolbox (http://web.mit.edu/swg/software.htm).

Outcome and Predictor Variables

To briefly reiterate, SPM8 first identified each voxel (within our anterior cerebral mask) whose connectivity (*z* score) with a specific seed correlated with a specific predictor (e.g., PCL-5) at $p < .001$. Such voxels, if contiguous, formed clusters of varying sizes (numbers of voxels). SnPM13 then determined the minimum size that a cluster must be to be certain at $p < .1$ (and usually $p < .05$) that this cluster was not a false positive. In the clusters that survived SnPM correction for FWE, *z* scores for each voxel were averaged. This mean *z* score was the primary outcome variable whose association with the predictor variable was then tested using simple regression.

To reduce type I error, a limited subset of variables predicting rs-FC was chosen, pre hoc, among the symptom and sleep measures (Table 1). These included PCL-5, CHI, actigraph and diary TST, SOL and SE, nightmares and bad dreams on a per-diary basis, and percent slow wave sleep (SWS%) and percent rapid eye movement sleep from ambulatory PSG. CHI was computed to assess PTSD hyperarousal symptoms separately from remaining PTSD symptoms (46). Actigraphy and sleep diaries captured objective and subjective habitual sleep quality, respectively. Combining bad dreams and nightmares allowed a larger number of participants with nonzero values (59 vs. 35), although zero values

were still included. From PSG, only SWS% and percent rapid eye movement sleep were examined, as these are the sleep stages from which the most prominent architectural anomalies are noted in the early posttrauma period as well as in diagnosed PTSD (16,61,62).

Statistical Analyses

Analyses performed in SPM8 are described above. IBM SPSS Version 24 software for Macintosh (IBM Corp., Armonk, NY) was used to perform simple regressions to examine the magnitude and direction of associations between predictor variables and mean *z* scores extracted from clusters that survived SnPM FWE correction. In regressions, $p < .05$ was considered statistically significant.

RESULTS

Mean values and range of demographic, PTSD symptom, and sleep variables are shown in Table 1. Predictors chosen pre hoc for correlation with rs-FC are indicated.

Higher PCL-5 and CHI were each associated with less rs-FC between the right amygdala seed and right middle frontal cortex (MFC). Using SPSS, simple regression analysis showed that both PCL-5 scores and CHI were negatively correlated with the right amygdala seed to right MFC mean *z* scores. No other regions associated with PTSD severity or CHI survived SnPM correction (Table 2 and Figure 1; Supplemental Table S3).

Higher actigraph TST was associated with less rs-FC between 1) left amygdala seed and dmPFC, 2) vmPFC seed and

Table 2. Correlation of Posttraumatic Symptoms, Sleep Quality, and Sleep Architecture Variables With Resting-State Connectivity of 5 Fear-Related and 1 Emotion Regulatory Seed Regions With Anterior Cerebral Voxel Clusters Surviving Familywise Error Correction Using SnPM

Predictor	Direction	Seed	Connected Regions With Seed	x, y, z (Peak Voxel)	Peak *t*	k[a]	Threshold k With SnPM[b]
Symptom							
PCL-5	Negative	Right amygdala	Right middle frontal cortex (BA 9)	40, 26, 24	4.33	365	204[d]
CHI	Negative	Right amygdala	Right middle frontal cortex (BA 9)	40, 26, 26	3.73	170	122[c]
Actigraphy							
Actigraph TST	Negative	Left amygdala	dmPFC (SMA; BA 8, BA 32, BA 6)	2, 18, 54	4.49	417	182[d]
	Negative	vmPFC	Right middle frontal cortex (BA 9, BA 10)	30, 34, 36	4.03	288	197[d]
	Positive	vmPFC	Left hippocampus	−20, −12, −20	4.02	313	183[d]
	Negative	Left amygdala	Right middle frontal cortex (BA 10)	38, 50, 20	3.73	173	113[c]
	Positive	vmPFC	Right hippocampus	24, −12, −20	3.85	161	126[c]
Actigraph SOL	Positive	dACC	Right posterior insular cortex (BA 13)	42, −10, 0	4.4	292	205[d]
	Positive	Left amygdala	Left insular cortex (BA 13)	−40, 6, −8	4.14	324	228[d]
	Positive	vmPFC	Right primary motor cortex (BA 4)	28, −24, 64	4.26	326	200[d]
	Positive	Left AIC	Right middle frontal cortex (BA 10)	30, 52, 14	3.76	233	206[d]
	Positive	dACC	Left posterior insular cortex (BA 13)	−40, −16, 2	3.67	153	134[c]
	Positive	Left amygdala	Right insular cortex (BA 13)	42, 8, −14	4.13	169	140[c]
Actigraph SE	Negative	vmPFC	SMA (BA 6)	2, −16, 72	4.52	636	184[d]
Diary							
Diary TST	Negative	Left AIC	Subgenual ACC (BA 25)	6, 12, −12	3.87	135	131[c]
	Positive	dACC	rACC (BA 24)	0, 30, 18	3.95	162	120[c]
Diary SOL	Positive	Right AIC	pre-SMA (BA 8, BA 6, BA 9)	−2, 42, 52	4.48	492	203[d]
	Positive	Right AIC	Left temporal pole (BA 38, BA 21)	−42, 18, −26	3.84	276	203[d]
Nightmare and bad dream rate	Positive	dACC	rACC (BA 24)	10, 32, −8	4.89	309	188[d]
	Positive	Left amygdala	Left primary motor cortex (BA 6, BA 4, BA 9)	−56, 0, 30	4.97	305	205[d]
	Negative	Left AIC	Left orbitofrontal cortex (BA 47)	−48, 28, 4	3.81	157	123[c]
	Positive	vmPFC	SMA (BA 6)	8, −8, 70	3.87	133	132[c]
PSG							
SWS%	Positive	Right amygdala	dmPFC (BA 8, BA 9)	−6, 28, 50	5.21	643	198[d]
	Positive	Right amygdala	rACC (BA 32)	8, 44, 8	4.14	218	198[d]

AIC, anterior insular cortex; BA, Brodmann area; CHI, composite hyperarousal index; dACC, dorsal anterior cingulate cortex; dmPFC, dorsomedial prefrontal cortex; PCL-5, PTSD Checklist for DSM-5; PSG, polysomnography; rACC, rostral anterior cingulate cortex; SE, sleep efficiency; SMA, supplementary motor area; SOL, sleep onset latency; SWS%, percent slow wave sleep; TST, total sleep time; vmPFC, ventromedial prefrontal cortex.

[a]The number of contiguous voxels in a cluster whose mean connectivity with the respective seed showed significant correlation with the respective sleep or symptom predictor variable using SPM.

[b]Minimum number of contiguous voxels in a cluster that the SnPM correction determined sufficiently large to not be a false positive at $p < .1$ or $p < .05$.

[c]$p < .1$.

[d]$p < .05$.

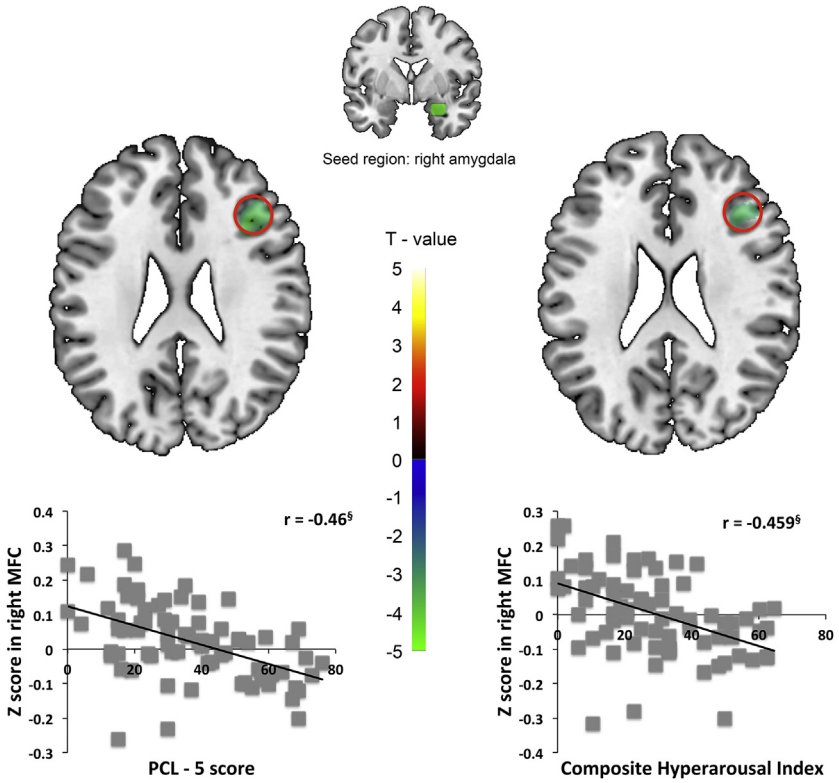

Figure 1. Posttraumatic stress disorder severity (PTSD Checklist for DSM-5 [PCL-5]) (left panel) and composite hyperarousal index (right panel) predict less resting-state functional connectivity between the right amygdala seed and the right middle frontal cortex (MFC). PCL-5 (left panel) and composite hyperarousal index (right panel) correlate negatively with extracted amygdala-MFC mean *z* values. §$p < .001$.

right MFC, and 3) left amygdala seed and right MFC. In contrast, higher actigraph TST was associated with greater rs-FC between vmPFC seed and bilateral hippocampus. Simple regression showed that actigraph TST was negatively correlated with 1) left amygdala seed to dmPFC, 2) vmPFC seed to right MFC, and 3) left amygdala seed to right MFC mean *z* scores. Actigraph TST was positively associated with vmPFC seed to bilateral hippocampus mean *z* scores. No other regions survived SnPM correction (Table 2 and Figure 2; Supplemental Table S3).

Higher actigraph SOL was associated with greater rs-FC between 1) dACC seed and bilateral posterior insular cortex, 2) left amygdala seed and bilateral insular cortex, 3) vmPFC seed and right primary motor cortex (M1), and 4) left AIC seed and right MFC. Simple regression showed that actigraph SOL was positively correlated with 1) dACC seed to right and left posterior insular cortex, 2) left amygdala seed to bilateral insular cortex, 3) vmPFC seed to right M1, and 4) left AIC seed to right MFC mean *z* scores. No other regions survived SnPM correction (Table 2; Supplemental Table S3 and Figure S2).

Higher actigraph SE was associated with less rs-FC between vmPFC seed and supplementary motor area (SMA). Simple regression analyses showed that actigraph SE was negatively correlated with vmPFC seed to SMA mean *z* scores. No other regions survived SnPM correction (Table 2; Supplemental Table S3 and Figure S3).

Higher diary TST was associated with less rs-FC between the left AIC seed and subgenual ACC. In contrast, higher diary TST was associated with greater rs-FC between the dACC seed and rACC. Simple regression analyses showed that diary TST was negatively correlated with dACC seed to subgenual ACC mean *z* scores and positively associated with dACC seed to rACC mean *z* scores. No other regions survived SnPM correction (Table 2; Supplemental Table S3 and Figure S4).

Higher diary SOL was associated with greater rs-FC between right AIC seed and 1) pre-SMA and 2) left temporal pole. Simple regression analyses showed that SOL was positively correlated with 1) right AIC seed to pre-SMA and 2) right AIC seed to right temporal pole mean *z* scores. No other regions survived SnPM correction (Table 2; Supplemental Table S3 and Figure S5).

A higher rate of combined nightmares and bad dreams was associated with less rs-FC between the left AIC seed and left orbitofrontal cortex, but greater rs-FC between 1) dACC seed and rACC, 2) left amygdala seed and left M1, and 3) vmPFC seed and SMA. Simple regression analyses showed that combined nightmare and bad dream rates were negatively correlated with left AIC seed to left orbitofrontal cortex mean *z* scores, but positively correlated with 1) dACC seed to rACC, 2) left amygdala seed to left M1, and 3) vmPFC seed to SMA mean *z* scores. No other regions survived SnPM correction (Table 2 and Figure 3; Supplemental Table S3).

Higher PSG SWS% was associated with greater rs-FC between right amygdala seed and 1) dmPFC and 2) rACC. Simple regression analyses showed that SWS% was positively correlated with 1) right amygdala seed to dmPFC and 2) right

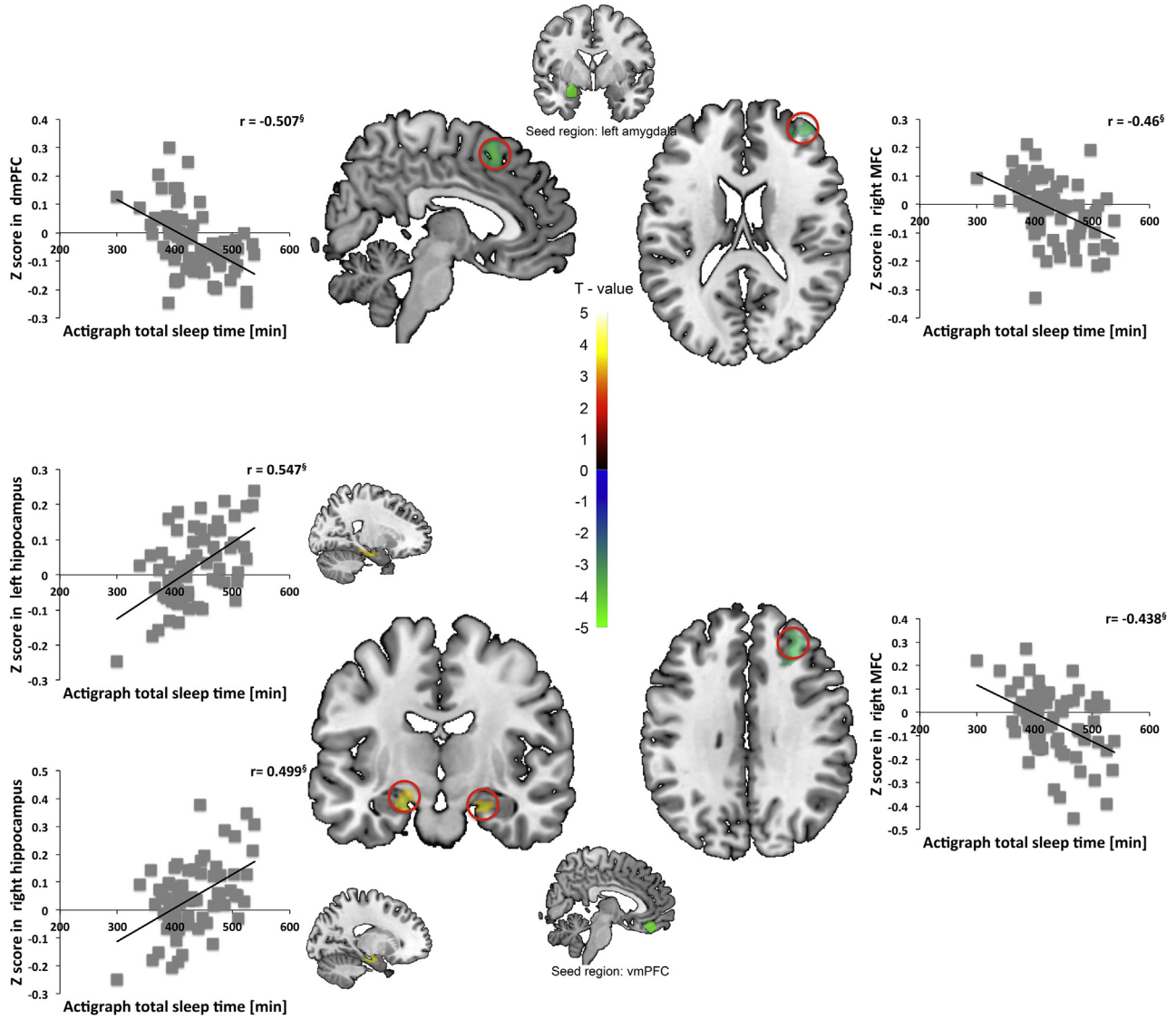

Figure 2. Actigraph total sleep time (TST) predicts less resting-state functional connectivity (rs-FC) between the left amygdala seed and the dorsomedial prefrontal cortex (dmPFC) and correlates negatively with extracted amygdala-dmPFC mean *z* values (upper left panel). TST predicts less rs-FC between the left amygdala seed and the right middle frontal cortex (MFC) and correlates negatively with extracted amygdala-MFC mean *z* values (upper right panel). TST predicts greater rs-FC between the ventromedial PFC (vmPFC) seed and bilateral hippocampi and correlates positively with extracted vmPFC-hippocampal mean *z* values (lower left panel). TST predicts less rs-FC between vmPFC seed and right MFC and correlates negatively with extracted vmPFC-MFC mean *z* values (lower right panel). §$p < .001$.

amygdala seed to rACC mean *z* scores. No other regions survived SnPM correction (Table 2 and Figure 4; Supplemental Table S3).

DISCUSSION

Greater actigraph SOL predicted greater connectivity between both the left amygdala and the dACC seeds with bilateral posterior insular cortex. As all these areas fall within the salience network, these findings support hypothesis 1.

PTSD symptom findings generally supported hypothesis 2, with both greater hyperarousal (CHI) and greater levels of total PTSD symptoms (PCL-5) predicting less rs-FC between the right amygdala seed and right MFC. (Note that after SnPM correction, both CHI and PCL-5 scores predicted this same rs-FC finding at an FWE of $p < .1$, but the PCL-5 score additionally predicted significance at $p < .05$.) PSG sleep architecture findings also supported hypothesis 2. Greater SWS% predicted greater connectivity between the right amygdala seed and the dmPFC and rACC. This latter finding is of particular interest as diminished SWS, relative to control subjects, was one of the few consistent sleep abnormalities reported in a meta-analysis of sleep studies in PTSD (61). Notably, SWS has been recently linked with emotional processing (63,64).

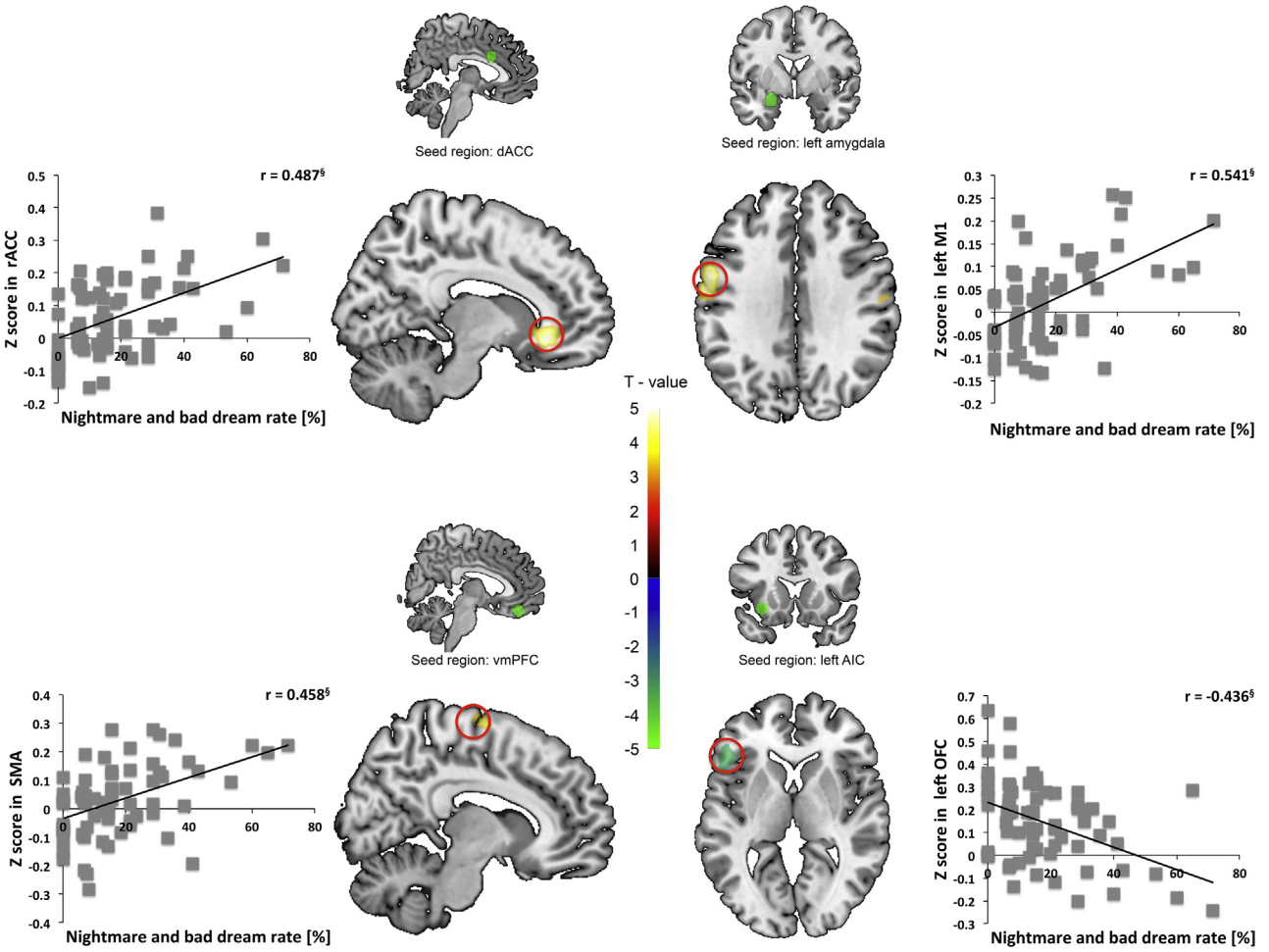

Figure 3. Nightmare and bad dream rate predicts greater resting-state functional connectivity (rs-FC) between the dorsal anterior cingulate cortex (dACC) seed and the rostral ACC (rACC) and correlates positively with extracted dACC-rACC mean *z* values (upper left panel). Nightmare and bad dream rate predicts greater rs-FC between the left amygdala seed and the left primary motor cortex (M1) and correlates positively with extracted amygdala-M1 mean *z* values (upper right panel). Nightmare and bad dream rate predicts more rs-FC between the ventromedial prefrontal cortex (vmPFC) seed and the supplementary motor cortex (SMA) and correlates positively with extracted vmPFC-SMA mean *z* values (lower left panel). Nightmare and bad dream rate predicts less rs-FC between left anterior insular cortex (AIC) seed and the left orbitofrontal cortex (OFC) and correlates negatively with extracted AIC-OFC mean *z* values (lower right panel). §$p < .001$.

In the case of habitual sleep measures, however, results were divided between those supporting and failing to support hypothesis 2. Greater diary TST predicted greater rs-FC between the dACC seed and the rACC, an emotion regulatory area (57,65,66), thus according with hypothesis 2. Similarly, a greater rate of nightmares predicted less rs-FC between the left AIC seed and the left orbitofrontal cortex. However, contradicting hypothesis 2, greater actigraph TST predicted less rs-FC between the left amygdala seed and the dmPFC and right MFC as well as less rs-FC between the vmPFC seed and the right MFC. Similarly, greater actigraph SOL predicted greater rs-FC between the left AIC seed and right MFC. Moreover, a greater rate of nightmares predicted greater rs-FC between the dACC seed and the rACC, and less diary TST predicted greater rs-FC between the left AIC seed and the subgenual ACC (Brodmann area 25), an area that has been linked with fear extinction (67).

Several predictors were associated with rs-FC between specific seeds and regions not clearly related to our 2 hypotheses, including the hippocampus, M1, SMA, pre-SMA, and temporal pole. The hippocampus is believed to provide contextual information that disambiguates potentially fearful situations, and as such, some investigators assign it an emotion regulatory role (8,14). If this is the case, the fact that greater actigraph TST predicted increased rs-FC between the vmPFC seed and bilateral hippocampi would support hypothesis 2.

Greater nightmare and bad dream rate predicted greater rs-FC between the left amygdala seed and left M1 Speculatively, this might represent greater readiness to react motorically to fear stimuli conveyed directly to the amygdala from the thalamus via the "low road" bypassing sensory and associative cortices (68). As such, this would support hypothesis 1.

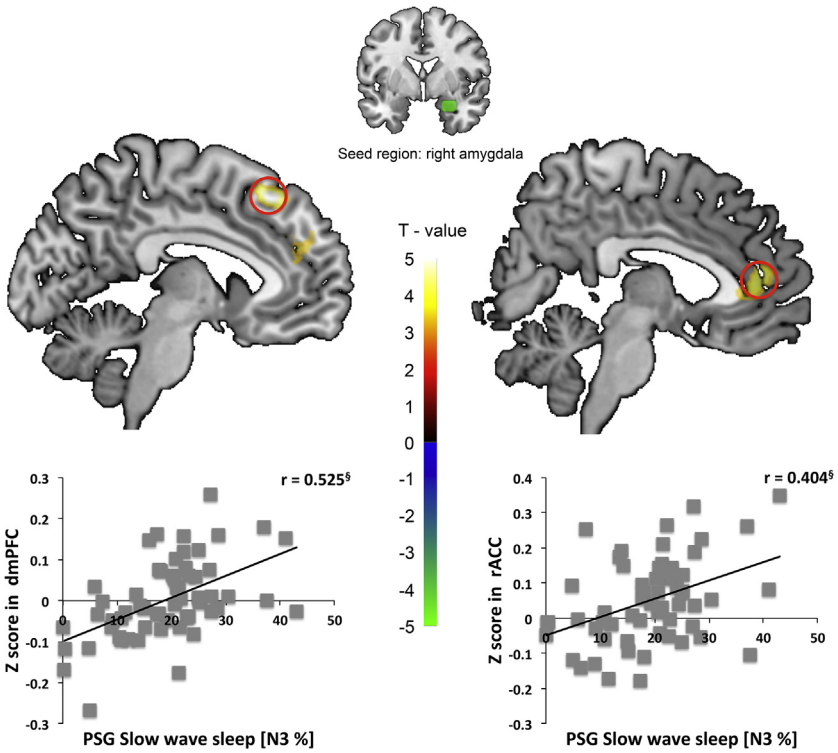

Figure 4. Percent slow wave sleep predicts greater resting-state functional connectivity between the right amygdala seed and the dorsomedial prefrontal cortex (dmPFC) and correlates positively with extracted amygdala-dmPFC mean z values (left panel). Percent slow wave sleep predicts greater resting-state functional connectivity between the right amygdala seed and the rostral anterior cingulate cortex (rACC) and correlates positively with extracted amygdala-rACC mean *z* values (right panel). §$p < .001$. PSG, polysomnography.

The SMA and particularly the pre-SMA are believed to be involved in motor control, specifically inhibition of ongoing motor sequences in service of initiating new behavior (69), possibly in response to detection of error or conflict (70). As such, these areas of the dmPFC may be considered to exert executive control. Thus, greater actigraph SE predicting less rs-FC between the vmPFC seed and SMA, greater nightmare rate predicting greater rs-FC between the vmPFC seed and SMA, and greater diary SOL predicting greater rs-FC between the right AIC seed and pre-SMA all would appear to contradict hypothesis 2. Nonetheless, other investigators have suggested the SMA and pre-SMA might be considered part of the salience network, given their putative functions in initiating and switching behavior in response to salient stimuli (30,71). From this viewpoint, the third (diary SOL) finding above would support hypothesis 1.

Lastly, the temporal pole (Brodmann area 38), although clearly an important limbic structure involved in socioemotional information processing (72), is not clearly involved in either the salience or the fear networks or in top-down control of emotion. Hence, its rs-FC is difficult to interpret relative to hypotheses 1 and 2.

A number of factors limit the generalizability of these findings. First, although a comparatively large sample was analyzed, it was not as large as might ultimately be required to maximize confidence in these findings, and we adopted an FWE threshold of $p < .1$ so as to avoid type II error. Second, seed-based rs-FC restricts analyses to connectivity with specified seed regions, and connectivity from adjacent regions having similar functional significance as these seeds is necessarily not sampled. A much larger sample, however, would be required to examine connectivity between every pair of voxels (31). Third, our sample is weighted toward young, female, educated, community-recruited individuals exposed to civilian trauma. Fourth, a 2-year window for an index trauma allows additional factors to intervene, including incident comorbidity and treatment. A sample obtained from a narrower window, although much more difficult to obtain, would provide greater confidence in the specific association of findings with the index trauma.

Conclusions

In individuals recently exposed to trauma and spanning the range from asymptomatic to a PTSD diagnosis, longer average objective SOL was associated with greater connectivity between fear-related seeds and other regions of the salience network. Greater waking symptoms were associated with less connectivity between fear-related seeds and anterior emotion regulatory regions, whereas greater SWS% was associated with more connectivity between these regions. Posttraumatic symptoms, including prolonged SOL, may reflect excessive activity in the salience network and less top-down control of this network by the PFC. Larger samples will be needed to further characterize correlates of rs-FC in this population.

ACKNOWLEDGMENTS AND DISCLOSURES

This work was supported by the National Institute of Mental Health (Grant No. R01MH109638 [to EFP-S]).

We thank Karen Gannon, RPSGT, for scoring sleep recordings and Cherrysse Ulsa and Sabrina Fleishaker for assistance with data reduction. Research was carried out at the Athinoula A. Martinos Center for Biomedical Imaging and the Psychiatric Neuroimaging Division, Department of Psychiatry, Massachusetts General Hospital, Charlestown, Massachusetts.

The authors report no biomedical financial interests or potential conflicts of interest.

ARTICLE INFORMATION

From the Department of Psychiatry and Athinoula A. Martinos Center for Biomedical Imaging, Massachusetts General Hospital; and Department of Psychiatry, Harvard Medical School, Charlestown, Massachusetts.

Address correspondence to Edward F. Pace-Schott, Ph.D., Harvard Medical School, Massachusetts General Hospital – East, CNY 149 13th Street, Room 2605, Charlestown, MA 02129; E-mail: epace-schott@mgh.harvard.edu.

Received Mar 29, 2019; revised Jun 24, 2019; accepted Jun 25, 2019.

Supplementary material cited in this article is available online at https://doi.org/10.1016/j.bpsc.2019.06.013.

REFERENCES

1. Germain A (2013): Sleep disturbances as the hallmark of PTSD: Where are we now? Am J Psychiatry 170:372–382.
2. Pigeon WR, Mellman TA (2017): Dreams and nightmares in posttraumatic stress disorder. In: Kryger MH, Roth T, Dement WC, editors. Principles and Practice of Sleep Medicine, 6th ed. Philadelphia: Elsevier, 561–566.
3. Pace-Schott EF, Bottary RM (2018): Characterization, conceptualization, and treatment of sleep disturbances in PTSD. In: Stoddard FJ Jr, Benedek DM, Milad MR, Ursano RJ, editors. Primer on Trauma- and Stressor-Related Disorders. New York: Oxford University Press, 148–160.
4. Marcks BA, Weisberg RB, Edelen MO, Keller MB (2010): The relationship between sleep disturbance and the course of anxiety disorders in primary care patients. Psychiatry Res 178:487–492.
5. Connelly M, Denney DR (2007): Regulation of emotions during experimental stress in alexithymia. J Psychosom Res 62:649–656.
6. Bardeen JR, Orcutt HK (2011): Attentional control as a moderator of the relationship between posttraumatic stress symptoms and attentional threat bias. J Anxiety Disord 25:1008–1018.
7. Cisler JM, Wolitzky-Taylor KB, Adams TG Jr, Babson KA, Badour CL, Willems JL (2011): The emotional Stroop task and posttraumatic stress disorder: a meta-analysis. Clin Psychol Rev 31:817–828.
8. Milad MR, Pitman RK, Ellis CB, Gold AL, Shin LM, Lasko NB, *et al.* (2009): Neurobiological basis of failure to recall extinction memory in posttraumatic stress disorder. Biol Psychiatry 66:1075–1082.
9. Fonzo GA, Simmons AN, Thorp SR, Norman SB, Paulus MP, Stein MB (2010): Exaggerated and disconnected insular-amygdalar blood oxygenation level-dependent response to threat-related emotional faces in women with intimate-partner violence posttraumatic stress disorder. Biol Psychiatry 68:433–441.
10. Shvil E, Rusch HL, Sullivan GM, Neria Y (2013): Neural, psychophysiological, and behavioral markers of fear processing in PTSD: A review of the literature. Curr Psychiatry Rep 15:358.
11. Morey RA, Dunsmoor JE, Haswell CC, Brown VM, Vora A, Weiner J, *et al.* (2015): Fear learning circuitry is biased toward generalization of fear associations in posttraumatic stress disorder. Transl Psychiatry 5:e700.
12. Lopresto D, Schipper P, Homberg JR (2016): Neural circuits and mechanisms involved in fear generalization: Implications for the pathophysiology and treatment of posttraumatic stress disorder. Neurosci Biobehav Rev 60:31–42.
13. Lazarov A, Suarez-Jimenez B, Tamman A, Falzon L, Zhu X, Edmondson DE, *et al.* (2019): Attention to threat in posttraumatic stress disorder as indexed by eye-tracking indices: A systematic review. Psychol Med 49:705–726.
14. Milad MR, Quirk GJ (2012): Fear extinction as a model for translational neuroscience: Ten years of progress. Annu Rev Psychol 63:129–151.
15. Shin LM, Liberzon I (2010): The neurocircuitry of fear, stress, and anxiety disorders. Neuropsychopharmacology 35:169–191.
16. Pace-Schott EF, Germain A, Milad MR (2015): Sleep and REM sleep disturbance in the pathophysiology of PTSD: The role of extinction memory. Biol Mood Anxiety Disord 5:3.
17. Rasch B, Born J (2013): About sleep's role in memory. Physiol Rev 93:681–766.
18. Goldstein AN, Walker MP (2014): The role of sleep in emotional brain function. Annu Rev Clin Psychol 10:679–708.
19. Pace-Schott EF, Germain A, Milad MR (2015): Effects of sleep on memory for conditioned fear and fear extinction. Psychol Bull 141:835–857.
20. Insel T, Cuthbert B, Garvey M, Heinssen R, Pine DS, Quinn K, *et al.* (2010): Research domain criteria (RDoC): Toward a new classification framework for research on mental disorders. Am J Psychiatry 167:748–751.
21. Etkin A, Wager TD (2007): Functional neuroimaging of anxiety: A meta-analysis of emotional processing in PTSD, social anxiety disorder, and specific phobia. Am J Psychiatry 164:1476–1488.
22. Greicius MD, Supekar K, Menon V, Dougherty RF (2009): Resting-state functional connectivity reflects structural connectivity in the default mode network. Cereb Cortex 19:72–78.
23. Hagmann P, Cammoun L, Gigandet X, Meuli R, Honey CJ, Wedeen VJ, *et al.* (2008): Mapping the structural core of human cerebral cortex. PLoS Biol 6:e159.
24. van den Heuvel MP, Mandl RC, Kahn RS, Hulshoff Pol HE (2009): Functionally linked resting-state networks reflect the underlying structural connectivity architecture of the human brain. Hum Brain Mapp 30:3127–3141.
25. Vincent JL, Patel GH, Fox MD, Snyder AZ, Baker JT, Van Essen DC, *et al.* (2007): Intrinsic functional architecture in the anaesthetized monkey brain. Nature 447:83–86.
26. Fox MD, Raichle ME (2007): Spontaneous fluctuations in brain activity observed with functional magnetic resonance imaging. Nat Rev 8:700–711.
27. Fox MD, Zhang D, Snyder AZ, Raichle ME (2009): The global signal and observed anticorrelated resting state brain networks. J Neurophysiol 101:3270–3283.
28. Raichle ME (2011): The restless brain. Brain Connect 1:3–12.
29. Peterson A, Thome J, Frewen P, Lanius RA (2014): Resting-state neuroimaging studies: A new way of identifying differences and similarities among the anxiety disorders? Can J Psychiatry 59:294–300.
30. Seeley WW, Menon V, Schatzberg AF, Keller J, Glover GH, Kenna H, *et al.* (2007): Dissociable intrinsic connectivity networks for salience processing and executive control. J Neurosci 27:2349–2356.
31. Yeo BT, Krienen FM, Sepulcre J, Sabuncu MR, Lashkari D, Hollinshead M, *et al.* (2011): The organization of the human cerebral cortex estimated by intrinsic functional connectivity. J Neurophysiol 106:1125–1165.
32. Nicholson AA, Sapru I, Densmore M, Frewen PA, Neufeld RW, Theberge J, *et al.* (2016): Unique insula subregion resting-state functional connectivity with amygdala complexes in posttraumatic stress disorder and its dissociative subtype. Psychiatry Res Neuroimaging 250:61–72.
33. Olson EA, Kaiser RH, Pizzagalli DA, Rauch SL, Rosso IM (2019): Regional prefrontal resting-state functional connectivity in posttraumatic stress disorder. Biol Psychiatry Cogn Neurosci Neuroimaging 4:390–398.
34. King AP, Block SR, Sripada RK, Rauch S, Giardino N, Favorite T, *et al.* (2016): Altered default mode network (DMN) resting state functional connectivity following a mindfulness-based exposure therapy for posttraumatic stress disorder (PTSD) in combat veterans of Afghanistan and Iraq. Depress Anxiety 33:289–299.
35. Koch SB, van Zuiden M, Nawijn L, Frijling JL, Veltman DJ, Olff M (2016): Aberrant resting-state brain activity in posttraumatic stress disorder: A meta-analysis and systematic review. Depress Anxiety 33:592–605.

36. Cuthbert BN (2014): The RDoC framework: Facilitating transition from ICD/DSM to dimensional approaches that integrate neuroscience and psychopathology. World Psychiatry 13:28–35.
37. Simpson HB (2012): The RDoC project: A new paradigm for investigating the pathophysiology of anxiety. Depress Anxiety 29:251–252.
38. Disner SG, Marquardt CA, Mueller BA, Burton PC, Sponheim SR (2018): Spontaneous neural activity differences in posttraumatic stress disorder: A quantitative resting-state meta-analysis and fMRI validation. Hum Brain Mapp 39:837–850.
39. Wang T, Liu J, Zhang J, Zhan W, Li L, Wu M, *et al.* (2016): Altered resting-state functional activity in posttraumatic stress disorder: A quantitative meta-analysis. Sci Rep 6:27131.
40. Rougemont-Bucking A, Linnman C, Zeffiro TA, Zeidan MA, Lebron-Milad K, Rodriguez-Romaguera J, *et al.* (2011): Altered processing of contextual information during fear extinction in PTSD: An fMRI study. CNS Neurosci Ther 17:227–236.
41. Milad MR, Rauch SL (2012): Obsessive-compulsive disorder: Beyond segregated cortico-striatal pathways. Trends Cogn Sci 16:43–51.
42. Ochsner KN, Gross JJ (2005): The cognitive control of emotion. Trends Cogn Sci 9:242–249.
43. Delgado MR, Nearing KI, Ledoux JE, Phelps EA (2008): Neural circuitry underlying the regulation of conditioned fear and its relation to extinction. Neuron 59:829–838.
44. First MB, Gibbon M, Spitzer RL, Williams JBW (2007): Structured Clinical Interview for DSM-IV-TR Axis I Disorders–Non-Patient Edition (SCID-I/NP). New York: Biometrics Research Department, New York State Psychiatric Institute.
45. Blake DD, Weathers FW, Nagy LM, Kaloupek DG, Gusman FD, Charney DS, *et al.* (1995): The development of a Clinician-Administered PTSD Scale. J Trauma Stress 8:75–90.
46. Blevins CA, Weathers FW, Davis MT, Witte TK, Domino JL (2015): The Posttraumatic Stress Disorder Checklist for DSM-5 (PCL-5): Development and initial psychometric evaluation. J Trauma Stress 28:489–498.
47. Kushida CA, Chang A, Gadkary C, Guilleminault C, Carrillo O, Dement WC (2001): Comparison of actigraphic, polysomnographic, and subjective assessment of sleep parameters in sleep-disordered patients. Sleep Med 2:389–396.
48. Lichstein KL, Stone KC, Donaldson J, Nau SD, Soeffing JP, Murray D, *et al.* (2006): Actigraphy validation with insomnia. Sleep 29:232–239.
49. Pace-Schott EF, Kaji J, Stickgold R, Hobson JA (1994): Nightcap measurement of sleep quality in self-described good and poor sleepers. Sleep 17:688–692.
50. Pace-Schott EF, Stickgold R, Muzur A, Wigren PE, Ward AS, Hart CL, *et al.* (2005): Sleep quality deteriorates over a binge-abstinence cycle in chronic smoked cocaine users. Psychopharmacology (Berl) 179:873–883.
51. Whitfield-Gabrieli S, Nieto-Castanon A (2012): Conn: A functional connectivity toolbox for correlated and anticorrelated brain networks. Brain Connect 2:125–141.
52. Behzadi Y, Restom K, Liau J, Liu TT (2007): A component based noise correction method (CompCor) for BOLD and perfusion based fMRI. Neuroimage 37:90–101.
53. Graham BM, Milad MR (2011): The study of fear extinction: Implications for anxiety disorders. Am J Psychiatry 168:1255–1265.
54. Tzourio-Mazoyer N, Landeau B, Papathanassiou D, Crivello F, Etard O, Delcroix N, *et al.* (2002): Automated anatomical labeling of activations in SPM using a macroscopic anatomical parcellation of the MNI MRI single-subject brain. Neuroimage 15:273–289.
55. Maldjian JA, Laurienti PJ, Kraft RA, Burdette JH (2003): An automated method for neuroanatomic and cytoarchitectonic atlas-based interrogation of fMRI data sets. Neuroimage 19:1233–1239.
56. Yarkoni T, Poldrack RA, Nichols TE, Van Essen DC, Wager TD (2011): Large-scale automated synthesis of human functional neuroimaging data. Nat Methods 8:665–670.
57. Pace-Schott EF, Zimmerman JP, Bottary RM, Lee EG, Milad MR, Camprodon JA (2017): Resting state functional connectivity in primary insomnia, generalized anxiety disorder and controls. Psychiatry Res Neuroimaging 265:26–34.
58. Whitfield-Gabrieli S, Moran JM, Nieto-Castanon A, Triantafyllou C, Saxe R, Gabrieli JD (2011): Associations and dissociations between default and self-reference networks in the human brain. Neuroimage 55:225–232.
59. Winkler AM, Ridgway GR, Webster MA, Smith SM, Nichols TE (2014): Permutation inference for the general linear model. Neuroimage 92:381–397.
60. Eklund A, Nichols TE, Knutsson H (2016): Cluster failure: Why fMRI inferences for spatial extent have inflated false-positive rates. Proc Natl Acad Sci U S A 113:7900–7905.
61. Kobayashi I, Boarts JM, Delahanty DL (2007): Polysomnographically measured sleep abnormalities in PTSD: A meta-analytic review. Psychophysiology 44:660–669.
62. Mellman TA, Bustamante V, Fins AI, Pigeon WR, Nolan B (2002): REM sleep and the early development of posttraumatic stress disorder. Am J Psychiatry 159:1696–1701.
63. Cairney SA, Durrant SJ, Power R, Lewis PA (2015): Complementary roles of slow-wave sleep and rapid eye movement sleep in emotional memory consolidation. Cereb Cortex 25:1565–1575.
64. Hauner KK, Howard JD, Zelano C, Gottfried JA (2013): Stimulus-specific enhancement of fear extinction during slow wave sleep. Nat Neurosci 16:1553–1555.
65. Dodhia S, Hosanagar A, Fitzgerald DA, Labuschagne I, Wood AG, Nathan PJ, *et al.* (2014): Modulation of resting-state amygdala-frontal functional connectivity by oxytocin in generalized social anxiety disorder. Neuropsychopharmacology 39:2061–2069.
66. Pizzagalli DA (2011): Frontocingulate dysfunction in depression: Toward biomarkers of treatment response. Neuropsychopharmacology 36:183–206.
67. Phelps EA, Delgado MR, Nearing KI, LeDoux JE (2004): Extinction learning in humans: Role of the amygdala and vmPFC. Neuron 43:897–905.
68. LeDoux JE (2000): Emotion circuits in the brain. Annu Rev Neurosci 23:155–184.
69. Nachev P, Kennard C, Husain M (2008): Functional role of the supplementary and pre-supplementary motor areas. Nat Rev Neurosci 9:856–869.
70. Ridderinkhof KR, Ullsperger M, Crone EA, Nieuwenhuis S (2004): The role of the medial frontal cortex in cognitive control. Science 306:443–447.
71. Bonnelle V, Ham TE, Leech R, Kinnunen KM, Mehta MA, Greenwood RJ, *et al.* (2012): Salience network integrity predicts default mode network function after traumatic brain injury. Proc Natl Acad Sci U S A 109:4690–4695.
72. Olson IR, Plotzker A, Ezzyat Y (2007): The enigmatic temporal pole: A review of findings on social and emotional processing. Brain 130:1718–1731.